BABAR-CONF-01/05
SLAC-PUB-8929
hep-ex/0107074
July, 2001

Study of *CP*-violating asymmetries in $B \to \pi^{\pm}\pi^{\mp}, K^{\pm}\pi^{\mp}$ decays

The *BABAR* Collaboration

July 26, 2001

Abstract

We present a preliminary measurement of the time-dependent *CP*-violating asymmetry parameters $S_{\pi\pi}$ and $C_{\pi\pi}$ in neutral B decays to the $\pi^{\pm}\pi^{\mp}$ *CP* eigenstate, and an updated preliminary measurement of the charge asymmetry $\mathcal{A}_{K\pi}$ in $B \to K^{\pm}\pi^{\mp}$ decays. Event yields and *CP*-violation parameters are determined simultaneously from a multidimensional unbinned maximum likelihood fit. In a data sample consisting of approximately 33 million $\Upsilon(4S) \to B\overline{B}$ decays collected with the *BABAR* detector at the SLAC PEP-II asymmetric B Factory, we find 65^{+12}_{-11} $\pi^{\pm}\pi^{\mp}$ and 217 ± 18 $K^{\pm}\pi^{\mp}$ candidates and measure $S_{\pi\pi} = 0.03^{+0.53}_{-0.56} \pm 0.11$, $C_{\pi\pi} = -0.25^{+0.45}_{-0.47} \pm 0.14$, and $\mathcal{A}_{K\pi} = -0.07 \pm 0.08 \pm 0.02$, where the first error is statistical and the second is systematic.

Submitted to the
20^{th} International Symposium on Lepton and Photon Interactions at High Energies,
7/23–7/28/2001, Rome, Italy

Stanford Linear Accelerator Center, Stanford University, Stanford, CA 94309

Work supported in part by Department of Energy contract DE-AC03-76SF00515.

The *BABAR* Collaboration,

B. Aubert, D. Boutigny, J.-M. Gaillard, A. Hicheur, Y. Karyotakis, J. P. Lees, P. Robbe, V. Tisserand

Laboratoire de Physique des Particules, F-74941 Annecy-le-Vieux, France

A. Palano

Università di Bari, Dipartimento di Fisica and INFN, I-70126 Bari, Italy

G. P. Chen, J. C. Chen, N. D. Qi, G. Rong, P. Wang, Y. S. Zhu

Institute of High Energy Physics, Beijing 100039, China

G. Eigen, P. L. Reinertsen, B. Stugu

University of Bergen, Inst. of Physics, N-5007 Bergen, Norway

B. Abbott, G. S. Abrams, A. W. Borgland, A. B. Breon, D. N. Brown, J. Button-Shafer, R. N. Cahn, A. R. Clark, M. S. Gill, A. V. Gritsan, Y. Groysman, R. G. Jacobsen, R. W. Kadel, J. Kadyk, L. T. Kerth, S. Kluth, Yu. G. Kolomensky, J. F. Kral, C. LeClerc, M. E. Levi, T. Liu, G. Lynch, A. B. Meyer, M. Momayezi, P. J. Oddone, A. Perazzo, M. Pripstein, N. A. Roe, A. Romosan, M. T. Ronan, V. G. Shelkov, A. V. Telnov, W. A. Wenzel

Lawrence Berkeley National Laboratory and University of California, Berkeley, CA 94720, USA

P. G. Bright-Thomas, T. J. Harrison, C. M. Hawkes, D. J. Knowles, S. W. O'Neale, R. C. Penny, A. T. Watson, N. K. Watson

University of Birmingham, Birmingham, B15 2TT, United Kingdom

T. Deppermann, K. Goetzen, H. Koch, J. Krug, M. Kunze, B. Lewandowski, K. Peters, H. Schmuecker, M. Steinke

Ruhr Universität Bochum, Institut für Experimentalphysik 1, D-44780 Bochum, Germany

J. C. Andress, N. R. Barlow, W. Bhimji, N. Chevalier, P. J. Clark, W. N. Cottingham, N. De Groot, N. Dyce, B. Foster, J. D. McFall, D. Wallom, F. F. Wilson

University of Bristol, Bristol BS8 1TL, United Kingdom

K. Abe, C. Hearty, T. S. Mattison, J. A. McKenna, D. Thiessen

University of British Columbia, Vancouver, BC, Canada V6T 1Z1

S. Jolly, A. K. McKemey, J. Tinslay

Brunel University, Uxbridge, Middlesex UB8 3PH, United Kingdom

V. E. Blinov, A. D. Bukin, D. A. Bukin, A. R. Buzykaev, V. B. Golubev, V. N. Ivanchenko, A. A. Korol, E. A. Kravchenko, A. P. Onuchin, A. A. Salnikov, S. I. Serednyakov, Yu. I. Skovpen, V. I. Telnov, A. N. Yushkov

Budker Institute of Nuclear Physics, Novosibirsk 630090, Russia

D. Best, A. J. Lankford, M. Mandelkern, S. McMahon, D. P. Stoker

University of California at Irvine, Irvine, CA 92697, USA

A. Ahsan, K. Arisaka, C. Buchanan, S. Chun

University of California at Los Angeles, Los Angeles, CA 90024, USA

J. G. Branson, D. B. MacFarlane, S. Prell, Sh. Rahatlou, G. Raven, V. Sharma

University of California at San Diego, La Jolla, CA 92093, USA

C. Campagnari, B. Dahmes, P. A. Hart, N. Kuznetsova, S. L. Levy, O. Long, A. Lu, J. D. Richman, W. Verkerke, M. Witherell, S. Yellin

University of California at Santa Barbara, Santa Barbara, CA 93106, USA

J. Beringer, D. E. Dorfan, A. M. Eisner, A. Frey, A. A. Grillo, M. Grothe, C. A. Heusch, R. P. Johnson, W. Kroeger, W. S. Lockman, T. Pulliam, H. Sadrozinski, T. Schalk, R. E. Schmitz, B. A. Schumm, A. Seiden, M. Turri, W. Walkowiak, D. C. Williams, M. G. Wilson

University of California at Santa Cruz, Institute for Particle Physics, Santa Cruz, CA 95064, USA

E. Chen, G. P. Dubois-Felsmann, A. Dvoretskii, D. G. Hitlin, S. Metzler, J. Oyang, F. C. Porter, A. Ryd, A. Samuel, M. Weaver, S. Yang, R. Y. Zhu

California Institute of Technology, Pasadena, CA 91125, USA

S. Devmal, T. L. Geld, S. Jayatilleke, G. Mancinelli, B. T. Meadows, M. D. Sokoloff

University of Cincinnati, Cincinnati, OH 45221, USA

T. Barillari, P. Bloom, M. O. Dima, S. Fahey, W. T. Ford, D. R. Johnson, U. Nauenberg, A. Olivas, H. Park, P. Rankin, J. Roy, S. Sen, J. G. Smith, W. C. van Hoek, D. L. Wagner

University of Colorado, Boulder, CO 80309, USA

J. Blouw, J. L. Harton, M. Krishnamurthy, A. Soffer, W. H. Toki, R. J. Wilson, J. Zhang

Colorado State University, Fort Collins, CO 80523, USA

T. Brandt, J. Brose, T. Colberg, G. Dahlinger, M. Dickopp, R. S. Dubitzky, A. Hauke, E. Maly, R. Müller-Pfefferkorn, S. Otto, K. R. Schubert, R. Schwierz, B. Spaan, L. Wilden

Technische Universität Dresden, Institut für Kern- und Teilchenphysik, D-01062, Dresden, Germany

L. Behr, D. Bernard, G. R. Bonneaud, F. Brochard, J. Cohen-Tanugi, S. Ferrag, E. Roussot, S. T'Jampens, Ch. Thiebaux, G. Vasileiadis, M. Verderi

Ecole Polytechnique, F-91128 Palaiseau, France

A. Anjomshoaa, R. Bernet, A. Khan, D. Lavin, F. Muheim, S. Playfer, J. E. Swain

University of Edinburgh, Edinburgh EH9 3JZ, United Kingdom

M. Falbo

Elon University, Elon University, NC 27244-2010, USA

C. Borean, C. Bozzi, S. Dittongo, M. Folegani, L. Piemontese

Università di Ferrara, Dipartimento di Fisica and INFN, I-44100 Ferrara, Italy

E. Treadwell

Florida A&M University, Tallahassee, FL 32307, USA

F. Anulli,[1] R. Baldini-Ferroli, A. Calcaterra, R. de Sangro, D. Falciai, G. Finocchiaro, P. Patteri, I. M. Peruzzi,[2]1 M. Piccolo, Y. Xie, A. Zallo

Laboratori Nazionali di Frascati dell'INFN, I-00044 Frascati, Italy

[1]Also with Università di Perugia, I-06100 Perugia, Italy

S. Bagnasco, A. Buzzo, R. Contri, G. Crosetti, P. Fabbricatore, S. Farinon, M. Lo Vetere, M. Macri, M. R. Monge, R. Musenich, M. Pallavicini, R. Parodi, S. Passaggio, F. C. Pastore, C. Patrignani, M. G. Pia, C. Priano, E. Robutti, A. Santroni

Università di Genova, Dipartimento di Fisica and INFN, I-16146 Genova, Italy

M. Morii

Harvard University, Cambridge, MA 02138, USA

R. Bartoldus, T. Dignan, R. Hamilton, U. Mallik

University of Iowa, Iowa City, IA 52242, USA

J. Cochran, H. B. Crawley, P.-A. Fischer, J. Lamsa, W. T. Meyer, E. I. Rosenberg

Iowa State University, Ames, IA 50011-3160, USA

M. Benkebil, G. Grosdidier, C. Hast, A. Höcker, H. M. Lacker, S. Laplace, V. Lepeltier, A. M. Lutz, S. Plaszczynski, M. H. Schune, S. Trincaz-Duvoid, A. Valassi, G. Wormser

Laboratoire de l'Accélérateur Linéaire, F-91898 Orsay, France

R. M. Bionta, V. Brigljević , D. J. Lange, M. Mugge, X. Shi, K. van Bibber, T. J. Wenaus, D. M. Wright, C. R. Wuest

Lawrence Livermore National Laboratory, Livermore, CA 94550, USA

M. Carroll, J. R. Fry, E. Gabathuler, R. Gamet, M. George, M. Kay, D. J. Payne, R. J. Sloane, C. Touramanis

University of Liverpool, Liverpool L69 3BX, United Kingdom

M. L. Aspinwall, D. A. Bowerman, P. D. Dauncey, U. Egede, I. Eschrich, N. J. W. Gunawardane, J. A. Nash, P. Sanders, D. Smith

University of London, Imperial College, London, SW7 2BW, United Kingdom

D. E. Azzopardi, J. J. Back, P. Dixon, P. F. Harrison, R. J. L. Potter, H. W. Shorthouse, P. Strother, P. B. Vidal, M. I. Williams

Queen Mary, University of London, E1 4NS, United Kingdom

G. Cowan, S. George, M. G. Green, A. Kurup, C. E. Marker, P. McGrath, T. R. McMahon, S. Ricciardi, F. Salvatore, I. Scott, G. Vaitsas

University of London, Royal Holloway and Bedford New College, Egham, Surrey TW20 0EX, United Kingdom

D. Brown, C. L. Davis

University of Louisville, Louisville, KY 40292, USA

J. Allison, R. J. Barlow, J. T. Boyd, A. C. Forti, J. Fullwood, F. Jackson, G. D. Lafferty, N. Savvas, E. T. Simopoulos, J. H. Weatherall

University of Manchester, Manchester M13 9PL, United Kingdom

A. Farbin, A. Jawahery, V. Lillard, J. Olsen, D. A. Roberts, J. R. Schieck

University of Maryland, College Park, MD 20742, USA

G. Blaylock, C. Dallapiccola, K. T. Flood, S. S. Hertzbach, R. Kofler, T. B. Moore, H. Staengle, S. Willocq

University of Massachusetts, Amherst, MA 01003, USA

B. Brau, R. Cowan, G. Sciolla, F. Taylor, R. K. Yamamoto
Massachusetts Institute of Technology, Laboratory for Nuclear Science, Cambridge, MA 02139, USA

M. Milek, P. M. Patel, J. Trischuk
McGill University, Montréal, Canada QC H3A 2T8

F. Lanni, F. Palombo
Università di Milano, Dipartimento di Fisica and INFN, I-20133 Milano, Italy

J. M. Bauer, M. Booke, L. Cremaldi, V. Eschenburg, R. Kroeger, J. Reidy, D. A. Sanders, D. J. Summers
University of Mississippi, University, MS 38677, USA

J. P. Martin, J. Y. Nief, R. Seitz, P. Taras, A. Woch, V. Zacek
Université de Montréal, Laboratoire René J. A. Lévesque, Montréal, Canada QC H3C 3J7

H. Nicholson, C. S. Sutton
Mount Holyoke College, South Hadley, MA 01075, USA

C. Cartaro, N. Cavallo,[3] G. De Nardo, F. Fabozzi, C. Gatto, L. Lista, P. Paolucci, D. Piccolo, C. Sciacca
Università di Napoli Federico II, Dipartimento di Scienze Fisiche and INFN, I-80126, Napoli, Italy

J. M. LoSecco
University of Notre Dame, Notre Dame, IN 46556, USA

J. R. G. Alsmiller, T. A. Gabriel, T. Handler
Oak Ridge National Laboratory, Oak Ridge, TN 37831, USA

J. Brau, R. Frey, M. Iwasaki, N. B. Sinev, D. Strom
University of Oregon, Eugene, OR 97403, USA

F. Colecchia, F. Dal Corso, A. Dorigo, F. Galeazzi, M. Margoni, G. Michelon, M. Morandin, M. Posocco, M. Rotondo, F. Simonetto, R. Stroili, E. Torassa, C. Voci
Università di Padova, Dipartimento di Fisica and INFN, I-35131 Padova, Italy

M. Benayoun, H. Briand, J. Chauveau, P. David, Ch. de la Vaissière, L. Del Buono, O. Hamon, F. Le Diberder, Ph. Leruste, J. Lory, L. Roos, J. Stark, S. Versillé
Universités Paris VI et VII, Lab de Physique Nucléaire H. E., F-75252 Paris, France

P. F. Manfredi, V. Re, V. Speziali
Università di Pavia, Dipartimento di Elettronica and INFN, I-27100 Pavia, Italy

E. D. Frank, L. Gladney, Q. H. Guo, J. H. Panetta
University of Pennsylvania, Philadelphia, PA 19104, USA

C. Angelini, G. Batignani, S. Bettarini, M. Bondioli, M. Carpinelli, F. Forti, M. A. Giorgi, A. Lusiani, F. Martinez-Vidal, M. Morganti, N. Neri, E. Paoloni, M. Rama, G. Rizzo, F. Sandrelli, G. Simi, G. Triggiani, J. Walsh
Università di Pisa, Scuola Normale Superiore and INFN, I-56010 Pisa, Italy

[3]Also with Università della Basilicata, I-85100 Potenza, Italy

M. Haire, D. Judd, K. Paick, L. Turnbull, D. E. Wagoner

Prairie View A&M University, Prairie View, TX 77446, USA

J. Albert, C. Bula, P. Elmer, C. Lu, K. T. McDonald, V. Miftakov, S. F. Schaffner, A. J. S. Smith, A. Tumanov, E. W. Varnes

Princeton University, Princeton, NJ 08544, USA

G. Cavoto, D. del Re, R. Faccini,[4] F. Ferrarotto, F. Ferroni, K. Fratini, E. Lamanna, E. Leonardi, M. A. Mazzoni, S. Morganti, G. Piredda, F. Safai Tehrani, M. Serra, C. Voena

Università di Roma La Sapienza, Dipartimento di Fisica and INFN, I-00185 Roma, Italy

S. Christ, R. Waldi

Universität Rostock, D-18051 Rostock, Germany

P. F. Jacques, M. Kalelkar, R. J. Plano

Rutgers University, New Brunswick, NJ 08903, USA

T. Adye, B. Franek, N. I. Geddes, G. P. Gopal, S. M. Xella

Rutherford Appleton Laboratory, Chilton, Didcot, Oxon, OX11 0QX, United Kingdom

R. Aleksan, G. De Domenico, S. Emery, A. Gaidot, S. F. Ganzhur, P.-F. Giraud, G. Hamel de Monchenault, W. Kozanecki, M. Langer, G. W. London, B. Mayer, B. Serfass, G. Vasseur, Ch. Yèche, M. Zito

DAPNIA, Commissariat à l'Energie Atomique/Saclay, F-91191 Gif-sur-Yvette, France

N. Copty, M. V. Purohit, H. Singh, F. X. Yumiceva

University of South Carolina, Columbia, SC 29208, USA

I. Adam, P. L. Anthony, D. Aston, K. Baird, J. P. Berger, E. Bloom, A. M. Boyarski, F. Bulos, G. Calderini, R. Claus, M. R. Convery, D. P. Coupal, D. H. Coward, J. Dorfan, M. Doser, W. Dunwoodie, R. C. Field, T. Glanzman, G. L. Godfrey, S. J. Gowdy, P. Grosso, T. Himel, T. Hryn'ova, M. E. Huffer, W. R. Innes, C. P. Jessop, M. H. Kelsey, P. Kim, M. L. Kocian, U. Langenegger, D. W. G. S. Leith, S. Luitz, V. Luth, H. L. Lynch, H. Marsiske, S. Menke, R. Messner, K. C. Moffeit, R. Mount, D. R. Muller, C. P. O'Grady, M. Perl, S. Petrak, H. Quinn, B. N. Ratcliff, S. H. Robertson, L. S. Rochester, A. Roodman, T. Schietinger, R. H. Schindler, J. Schwiening, V. V. Serbo, A. Snyder, A. Soha, S. M. Spanier, J. Stelzer, D. Su, M. K. Sullivan, H. A. Tanaka, J. Va'vra, S. R. Wagner, A. J. R. Weinstein, W. J. Wisniewski, D. H. Wright, C. C. Young

Stanford Linear Accelerator Center, Stanford, CA 94309, USA

P. R. Burchat, C. H. Cheng, D. Kirkby, T. I. Meyer, C. Roat

Stanford University, Stanford, CA 94305-4060, USA

R. Henderson

TRIUMF, Vancouver, BC, Canada V6T 2A3

W. Bugg, H. Cohn, A. W. Weidemann

University of Tennessee, Knoxville, TN 37996, USA

[4]Also with University of California at San Diego, La Jolla, CA 92093, USA

J. M. Izen, I. Kitayama, X. C. Lou, M. Turcotte
University of Texas at Dallas, Richardson, TX 75083, USA

F. Bianchi, M. Bona, B. Di Girolamo, D. Gamba, A. Smol, D. Zanin
Università di Torino, Dipartimento di Fisica Sperimentale and INFN, I-10125 Torino, Italy

L. Bosisio, G. Della Ricca, L. Lanceri, A. Pompili, P. Poropat, M. Prest, E. Vallazza, G. Vuagnin
Università di Trieste, Dipartimento di Fisica and INFN, I-34127 Trieste, Italy

R. S. Panvini
Vanderbilt University, Nashville, TN 37235, USA

C. M. Brown, A. De Silva, R. Kowalewski, J. M. Roney
University of Victoria, Victoria, BC, Canada V8W 3P6

H. R. Band, E. Charles, S. Dasu, F. Di Lodovico, A. M. Eichenbaum, H. Hu, J. R. Johnson, R. Liu, J. Nielsen, Y. Pan, R. Prepost, I. J. Scott, S. J. Sekula, J. H. von Wimmersperg-Toeller, S. L. Wu, Z. Yu, H. Zobernig
University of Wisconsin, Madison, WI 53706, USA

T. M. B. Kordich, H. Neal
Yale University, New Haven, CT 06511, USA

1 Introduction

In the Standard Model, all *CP*-violating effects arise from a single complex phase in the three-generation CKM quark-mixing matrix [1]. One of the central questions in particle physics is whether this mechanism is sufficient to explain the pattern of *CP* violation observed in nature. Recent measurements of the parameter sin2β by the *BABAR* [2] and BELLE [3] Collaborations establish that *CP* symmetry is violated in the neutral B-meson system. These measurements are in agreement with other direct measurements [4], as well as indirect constraints implied by measurements and theoretical estimates of the CKM matrix elements [5]. In addition to measuring sin2β more precisely, one of the primary goals of the B-Factory experiments in the future will be to measure the remaining angles (α and γ) and sides of the Unitarity Triangle in order to further test whether the Standard Model description of *CP* violation is correct.

The study of B decays to charmless hadronic two-body final states will play an increasingly important role in our understanding of *CP* violation. In the Standard Model, the time-dependent *CP*-violating asymmetry in the reaction $B \to \pi^+\pi^-$ is related to the angle α. In addition, observation of a significant asymmetry between the decay rates for $B^0 \to K^+\pi^-$ and $\overline{B}^0 \to K^-\pi^+$ would be evidence for direct *CP* violation, and ratios of branching fractions for various $\pi\pi$ and $K\pi$ decay modes are sensitive to the angle γ. Finally, branching fraction measurements provide critical tests of theoretical models that are needed to extract *CP* information from the experimental observables.

The *BABAR* Collaboration recently reported measurements of branching fractions and charge asymmetries for several charmless two-body B decays using a dataset of 22.6 million $B\overline{B}$ pairs [6]. In this paper, using a data sample of approximately 33 million $B\overline{B}$ pairs, we report preliminary measurements of the time-dependent *CP*-violating asymmetry in neutral B decays to the $\pi^+\pi^-$ *CP* eigenstate, and the asymmetry between $B^0 \to K^+\pi^-$ and $\overline{B}^0 \to K^-\pi^+$ decays.

2 Data sample and *BABAR* detector

The data sample used in this analysis consists of $33.7\,\mathrm{fb}^{-1}$ collected with the *BABAR* detector at the Stanford Linear Accelerator Center's PEP-II storage ring between October 1999 and June 2001. The PEP-II facility operates nominally at the $\Upsilon(4S)$ resonance, providing asymmetric collisions of 9.0 GeV electrons on 3.1 GeV positrons. The dataset includes $30.4\,\mathrm{fb}^{-1}$ collected in this configuration (on-resonance) and $3.3\,\mathrm{fb}^{-1}$ collected below the $B\overline{B}$ threshold (off-resonance) that are used for continuum background studies. The on-resonance sample corresponds to approximately 33 million produced $B\overline{B}$ pairs.

BABAR is a 4π solenoidal spectrometer optimized for the asymmetric beam configuration and is described in detail elsewhere [12]. Charged particle (track) momenta are measured in a tracking system consisting of a 5-layer, double-sided, silicon vertex tracker (SVT) and a 40-layer drift chamber (DCH) filled with a gas mixture of helium and isobutane, both operating within a 1.5 T superconducting solenoidal magnet. The typical decay vertex resolution for fully reconstructed B decays is approximately 65 μm along the center-of-mass (CM) boost direction. Photons are detected in an electromagnetic calorimeter (EMC) consisting of 6580 CsI(Tl) crystals arranged in barrel and forward endcap subdetectors. The iron flux return (IFR) is segmented and instrumented with multiple layers of resistive plate chambers for the identification of muons and long-lived neutral hadrons.

Tracks from the decay $B \to h^+h'^-$ are identified as pions or kaons by the Cherenkov angle θ_c measured by a detector of internally reflected Cherenkov light (DIRC). The DIRC system is a

unique type of Cherenkov detector that relies on total internal reflection within the radiator to deliver the Cherenkov light outside the tracking and magnetic volumes. The typical separation between pions and kaons varies from 8σ at $2\,\mathrm{GeV}/c$ to 2.5σ at $4\,\mathrm{GeV}/c$, where σ is the average resolution on θ_c. Kaons used in B tagging are identified with a combination of θ_c (for momenta down to $0.7\,\mathrm{GeV}/c$) and specific ionization (dE/dx) measurements in the DCH and SVT.

3 Analysis overview

The time-dependent *CP*-violating asymmetry in the decay $B \to \pi^+\pi^-$ arises from interference between mixing and decay amplitudes, and interference between the tree and penguin decay amplitudes. A $B^0\overline{B}^0$ pair produced in $\Upsilon(4S)$ decay evolves in time in a coherent P-wave state until one of the two mesons decays. We reconstruct the decay $B \to h^+h'^-$ (B_{hh}), where h is a pion or kaon, and examine the remaining particles in the event to "tag" the flavor of the other B meson ($B_{\rm tag}$). Defining $\Delta t = t_{hh} - t_{\rm tag}$ as the time between the decays of B_{hh} and $B_{\rm tag}$, the decay rate distribution $f_+\,(f_-)$ when $B_{hh} \to \pi^+\pi^-$ and $B_{\rm tag}$ is a $B^0\,(\overline{B}^0)$ is given by [5]

$$f_\pm(\Delta t) = \frac{e^{-|\Delta t|/\tau}}{4\tau}\left[1 \pm S_{\pi\pi}\sin(\Delta m_d \Delta t) \mp C_{\pi\pi}\cos(\Delta m_d \Delta t)\right], \tag{1}$$

where τ is the B^0 lifetime, Δm_d is the $B^0\overline{B}^0$ mixing frequency, and

$$S_{\pi\pi} = \frac{2\,\mathcal{I}m\lambda}{1+|\lambda|^2}, \quad \text{and,} \quad C_{\pi\pi} = \frac{1-|\lambda|^2}{1+|\lambda|^2}. \tag{2}$$

Ignoring the contribution from the penguin amplitude, the complex parameter λ is

$$\lambda(B \to \pi^+\pi^-) \equiv \frac{q}{p}\frac{\bar{A}_{\pi\pi}}{A_{\pi\pi}} = \eta_{\pi\pi}\left(\frac{V_{tb}^*V_{td}}{V_{tb}V_{td}^*}\right)\left(\frac{V_{ud}^*V_{ub}}{V_{ud}V_{ub}^*}\right), \tag{3}$$

where $\eta_{\pi\pi} = +1$ is the *CP* eigenvalue of the final state, and the assumption of no *CP* violation in mixing ($|q/p| = 1$) is implicit. Thus, in the absence of penguins, $|\lambda| = 1$ and $\mathcal{I}m\lambda = \sin 2\alpha$, where $\alpha \equiv \arg\left[-V_{td}V_{tb}^*/V_{ud}V_{ub}^*\right]$. However, the $b \to d$ gluonic penguin amplitude carries the weak phase $\arg(V_{td}^*V_{tb})$ and, in general, modifies both $|\lambda|$ and $\mathcal{I}m\lambda$. In this case, $|\lambda| \neq 1$ and $S_{\pi\pi}$ becomes

$$S_{\pi\pi} = \frac{2\,|\lambda|\sin 2\alpha_{\rm eff}}{1+|\lambda|^2}, \tag{4}$$

where $\alpha_{\rm eff}$ depends on the magnitudes and strong phases of the tree and penguin amplitudes. Recent theoretical estimates of the relative size of penguin and tree amplitudes vary [7, 8], but large effects are possible.

It is possible to extract α in the presence of penguins with little or no theoretical error using an isospin analysis [9] (see, however, Ref. [10]). The analysis requires measurements of the separate branching fractions for $B^0 \to \pi^0\pi^0$ and $\overline{B}^0 \to \pi^0\pi^0$ as well as the charge-averaged branching fraction for $B^\pm \to \pi^\pm\pi^0$. However, it will be some time before such an analysis is experimentally feasible. Alternatively, bounds on the penguin-induced shift in α can be derived from ratios of various two-body branching fractions [11]. Finally, recent theoretical work allows the extraction of α given a measurement of $S_{\pi\pi}$ [7].

[5] We assume $\Delta\Gamma = 0$.

In this analysis we extract signal and background yields for $\pi^\pm\pi^\mp$, $K^\pm\pi^\mp$, and $K^\pm K^\mp$ decays, and the amplitudes of the $\pi\pi$ sine ($S_{\pi\pi}$) and cosine ($C_{\pi\pi}$) oscillation terms simultaneously from an unbinned maximum likelihood fit. We parameterize the $K\pi$ component in terms of the total yield and the *CP*-violating charge asymmetry

$$\mathcal{A}_{K\pi} \equiv \frac{N_{K^-\pi^+} - N_{K^+\pi^-}}{N_{K^-\pi^+} + N_{K^+\pi^-}}. \tag{5}$$

Including the more abundant $K\pi$ sample in the fit also allows for validation of the Δt parameterization from direct measurements of τ and Δm_d (via mixing in $B^0 \to \overline{B}^0 \to K^-\pi^+$) in the same sample used to extract $S_{\pi\pi}$ and $C_{\pi\pi}$. In addition, background discrimination provided by the measurement of Δt improves the error on signal yields. The combined fit to yields and *CP* parameters therefore facilitates the simultaneous optimization of branching fraction and *CP* measurements, both of which are necessary to extract reliable information about α.

4 Event selection

Hadronic events are selected based on track multiplicity and event topology. Tracks in the polar angle region $0.41 < \theta_{\rm lab} < 2.54$ with transverse momentum greater than $100\,{\rm MeV}/c$ are required to pass quality cuts, including number of drift chamber hits used in the track fit and impact parameter in the r–ϕ and r–z planes, where the cylindrical coordinate z is aligned along the detector axis in the electron beam direction. At least three tracks must pass the above selection. To reduce contamination from Bhabha and $\mu^+\mu^-$ events the ratio of second to zeroth Fox-Wolfram moments [13], $R_2 = H_2/H_0$, is required to be less than 0.95. Residual background from tau hadronic decays is reduced by requiring the sphericity [14] of the event to be greater than 0.01.

Candidate $B \to h^+h'^-$ decays are reconstructed by combining pairs of oppositely-charged tracks (pion mass assumed) with a good quality vertex. We require each track to have an associated θ_c measurement with a minimum of six Cherenkov photons above background. Protons are rejected based on θ_c and electrons are rejected based on dE/dx, shower shape in the EMC, and the ratio of shower energy and track momentum. Non-resonant $q\bar{q}$ background is suppressed by removing jet-like events from the sample: we define the CM angle θ_S between the sphericity axes of the B candidate and the remaining tracks and photons in the event, and require $|\cos\theta_S| < 0.8$, which removes approximately 83% of the background. The total efficiency of the above selection on signal events is approximately 38%.

We define a beam-energy substituted mass $m_{\rm ES} = \sqrt{E_{\rm b}^2 - \mathbf{p}_B^2}$. The beam energy is defined in the laboratory frame as $E_{\rm b} = (s/2 + \mathbf{p}_i\cdot\mathbf{p}_B)/E_i$, where $\sqrt{s}$ and E_i are the total energies of the e^+e^- system in the CM and lab frames, respectively, and $\mathbf{p}_i$ and $\mathbf{p}_B$ are the momentum vectors in the lab frame of the e^+e^- system and the B candidate, respectively. Defining $m_{\rm ES}$ in the laboratory frame removes the dependence on the track mass hypothesis. Signal events are Gaussian distributed in $m_{\rm ES}$ with a mean of $5.280\,{\rm GeV}/c^2$ and a resolution of $2.6\,{\rm MeV}/c^2$. The background shape is parameterized by a threshold function [15] with a fixed endpoint given by the average beam energy.

We define a second kinematic variable ΔE as the difference between the B candidate energy in the CM frame and $\sqrt{s}/2$. The ΔE distribution is peaked near zero for $\pi^+\pi^-$ decays and shifted on average $-45\,{\rm MeV}$ ($-91\,{\rm MeV}$) for modes with one (two) charged kaons, where the exact separation depends on the laboratory kaon momentum. The resolution on ΔE for signal decays is approximately $26\,{\rm MeV}$. The background is parameterized by a quadratic function.

Candidate B mesons selected in the region $5.2 < m_{\rm ES} < 5.3\,{\rm GeV}/c^2$ and $|\Delta E| < 0.15\,{\rm GeV}$ are used to extract yields and *CP* parameters from an unbinned maximum likelihood fit. The total number of events in the fit region satisfying the above criteria is 9741. A sideband region, defined as $5.2 < m_{\rm ES} < 5.26\,{\rm GeV}/c^2$ and $|\Delta E| < 0.42\,{\rm GeV}$, is used to extract various background parameters.

5 Analysis

The analysis method combines the techniques used to measure charmless two-body branching fractions [6] and the *CP*-violating parameter sin2β [2]. The primary issues are

- determining the flavor of the $B_{\rm tag}$ meson;
- measuring the distance Δz between the B_{hh} and $B_{\rm tag}$ vertices;
- discriminating signal from background;
- separating pions and kaons in the kinematically similar decays $B \to \pi\pi$, $K\pi$, KK;
- extracting yields and *CP* asymmetries with an unbinned maximum likelihood fit;

The first four issues have been described in previous publications. In this section we summarize the main points and describe the fit technique.

5.1 Flavor tagging

We use the standard *BABAR* B-tagging algorithm to determine the flavor of the $B_{\rm tag}$ meson [16]. The algorithm relies on the correlation between the flavor of the b-quark and the charge of the remaining tracks in the event after removal of the B_{hh} candidate. Five mutually exclusive tagging categories are defined: `Lepton`, `Kaon`, `NT1`, `NT2`, and `Untagged`. `Lepton` tags rely on primary electrons and muons from semileptonic B decays, while `Kaon` tags use the sum of the charges of all identified kaons. The `NT1` and `NT2` categories are derived from a neural network that is sensitive to charge correlations between the parent B and unidentified leptons and kaons, soft pions, or the charge and momentum of the track with the highest CM momentum. The addition of `Untagged` events improves the signal yield estimates and provides a large sample for determinating background shape parameters directly in the maximum likelihood fit.

The quality of tagging is expressed in terms of the effective efficiency $Q = \sum_i \epsilon_i D_i^2$, where ϵ_i is the fraction of events tagged in category i and the dilution $D_i = 1 - 2w_i$ is related to the mistag fraction w_i. The statistical errors on $S_{\pi\pi}$ and $C_{\pi\pi}$ are proportional to $1/\sqrt{Q}$. Table 1 summarizes the tagging performance in $B\overline{B}$ events, obtained from a sample $B_{\rm flav}$ of fully reconstructed neutral B decays into $D^{(*)-}h^+$ ($h^+ = \pi^+, \rho^+, a_1^+$) and $J/\psi\,K^{*0}$ ($K^{*0} \to K^+\pi^-$) flavor eigenstates [2]. We use the same tagging efficiencies and dilutions for signal $\pi\pi$, $K\pi$, and KK decays. Separate background tagging efficiencies for each species are obtained from a fit to the on-resonance sideband data and reported in Table 2. The division of data into tagging category and flavor is summarized in Table 3, and the distributions of $m_{\rm ES}$ for events tagged in each category are shown in Fig. 1.

5.2 Resolution function for Δt

The time difference Δt is obtained from the measured distance between the z position of the B_{hh} and $B_{\rm tag}$ vertices and the known boost of the CM frame. The z position of the $B_{\rm tag}$ vertex

Table 1: Tagging efficiency, average dilution, dilution difference $\Delta D = D(B^0) - D(\overline{B}^0)$, and effective tagging efficiency Q for signal events in each tagging category, as measured in a sample of neutral B decays to flavor eigenstates.

Category	$\epsilon\,(\%)$	$D\,(\%)$	$\Delta D\,(\%)$	$Q\,(\%)$
`Lepton`	11.0 ± 0.3	82.3 ± 2.7	-2.1 ± 4.5	7.5 ± 0.5
`Kaon`	35.8 ± 0.5	64.8 ± 2.0	3.5 ± 3.1	15.0 ± 1.0
`NT1`	8.0 ± 0.3	55.6 ± 4.2	-12.1 ± 6.7	2.5 ± 0.4
`NT2`	13.9 ± 0.4	30.2 ± 3.8	9.0 ± 5.7	1.3 ± 0.3
`Untagged`	31.3 ± 0.5	–	–	–
Total Q				26.3 ± 1.2

Table 2: Tagging efficiencies (%) for background (b) events in each species ($\pi\pi, K\pi, KK$) as determined from a fit to the on-resonance sideband data.

Category	$\epsilon_b(\pi\pi)$	$\epsilon_b(K\pi)$	$\epsilon_b(KK)$
`Lepton`	1.0 ± 0.1	1.0 ± 0.1	1.5 ± 0.2
`Kaon`	26.0 ± 0.4	33.1 ± 0.6	23.5 ± 0.7
`NT1`	6.6 ± 0.2	5.4 ± 0.3	6.9 ± 0.4
`NT2`	17.6 ± 0.4	15.3 ± 0.5	19.7 ± 0.6
`Untagged`	48.9 ± 0.7	45.2 ± 0.6	48.3 ± 0.8

Table 3: Event yields in the 1999–2000 and 2001 datasets separated by tagging flavor and category.

	1999–2000			2001			Total		
Category	B^0	$\overline{B}^0$	Tot	B^0	$\overline{B}^0$	Tot	B^0	$\overline{B}^0$	Tot
Lepton	50	59	109	25	21	46	75	80	155
Kaon	920	877	1797	455	468	923	1375	1345	2720
NT1	215	195	410	107	92	199	322	287	609
NT2	621	560	1181	312	236	548	933	796	1729
Untagged	–	–	3103	–	–	1425	–	–	4528
Total	1806	1691	6600	899	817	3141	2705	2508	9741

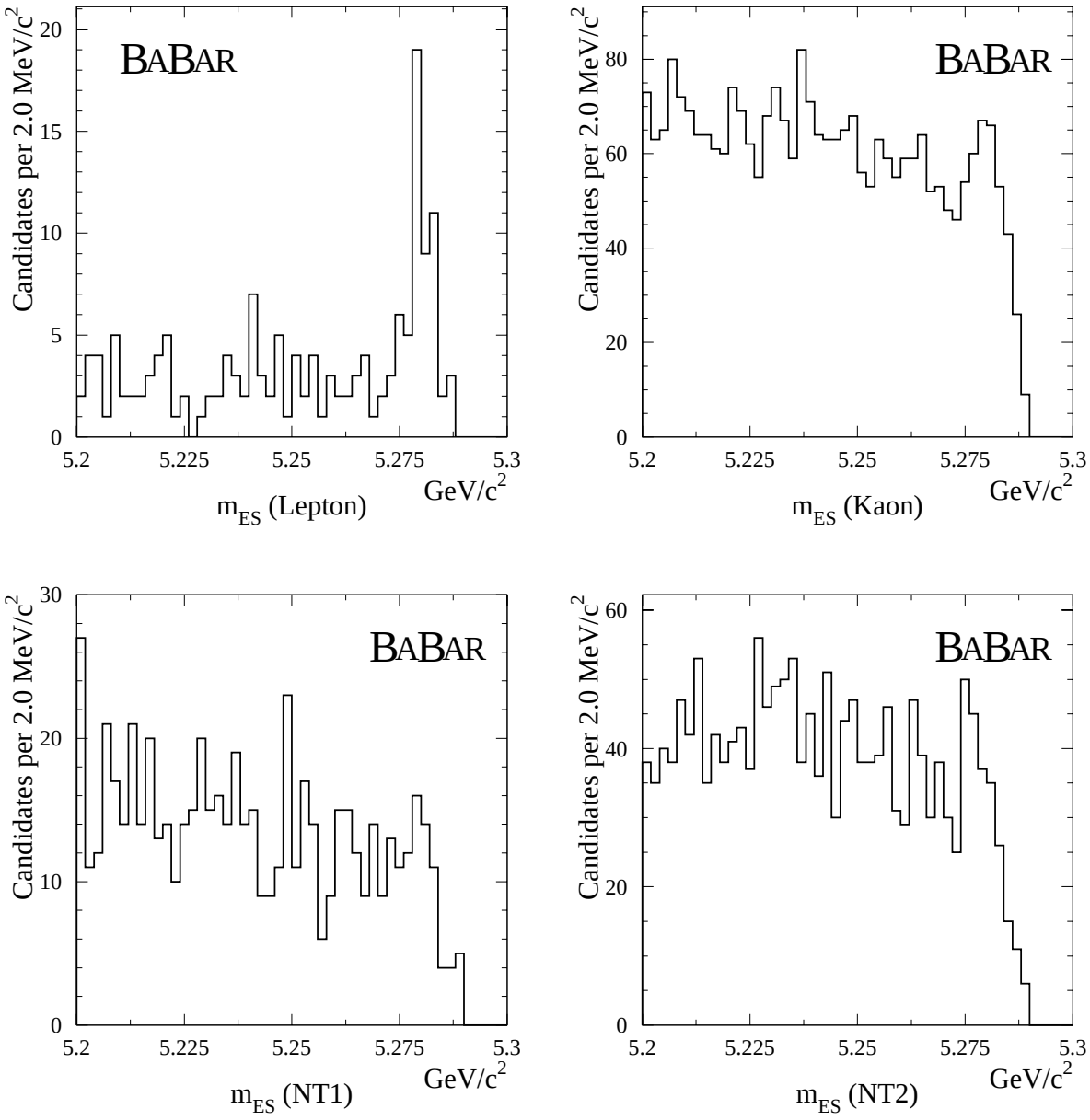

Figure 1: Distributions of $m_{\rm ES}$ for $h^+h'^-$ events satisfying the selection criteria and tagged in the `Lepton`, `Kaon`, `NT1`, and `NT2` categories.

is determined with an iterative procedure that removes tracks with a large contribution to the total χ^2 [2, 16]. An additional constraint is constructed from the three-momentum and vertex position of the B_{hh} candidate, and the average e^+e^- interaction point and boost. The typical Δz resolution is $180\,\mu$m. We require $|\Delta t| < 17\,$ps and $0.3 < \sigma_{\Delta t} < 3.0\,$ps, where $\sigma_{\Delta t}$ is the event-by-event error on Δt. The resolution function for signal candidates is identical to the one described in Ref. [2], with parameters determined from a fit to the combined tagged and untagged $B_{\rm flav}$ sample. The background resolution function is parameterized as the sum of three Gaussians, with the parameters determined from a fit to the on-resonance sideband data. For both signal and background, the resolution function parameters are different for data collected in 1999–2000 and 2001 due to improved alignment of the SVT in more recent data.

5.3 Background discrimination

The selected data sample contains 97% background, mostly due to random combinations of tracks produced in $e^+e^- \to q\bar{q}$ events ($q = u, d, s, c$). Discrimination of signal from background in the maximum likelihood fit is enhanced by the use of a Fisher discriminant $\mathcal{F}$ [6]. The Fisher variables are constructed from the scalar sum of the CM momenta of all tracks and photons (excluding tracks from the B_{hh} candidate) entering nine concentric cones centered on the thrust axis of the B_{hh} candidate. Background events dominantly contribute to the cones closest to the thrust axis, while the more spherical $B\overline{B}$ events distribute momentum more evenly. The distribution of $\mathcal{F}$ for signal events is parameterized as a single Gaussian, with parameters determined from Monte Carlo simulated decays and validated with data $B^- \to D^0\pi^-$ decays. The background shape is parameterized as the sum of two Gaussians, with parameters determined directly in the maximum likelihood fit.

5.4 Particle identification

Identification of B_{hh} tracks as pions or kaons is accomplished with the Cherenkov angle measurement from the DIRC. We construct Gaussian probability density functions (PDFs) from the difference between measured and expected values of θ_c for the pion or kaon hypothesis, normalized by the resolution. The DIRC performance is parameterized using a data sample of $D^{*+} \to D^0\pi^+$, $D^0 \to K^-\pi^+$ decays. Within the statistical precision of the control sample, we find similar response for positive and negative tracks and use a single parameterization for both. The performance of the DIRC has improved in the 2001 dataset due to a better aligned detector and improvements in the θ_c reconstruction algorithm. We therefore use different parameter sets for the two running periods.

5.5 Fit technique

We use an unbinned extended maximum likelihood fit to extract yields and *CP* parameters from the $h^+h'^-$ sample. The likelihood for candidate j tagged in category c is obtained by summing the product of event yield n_i, tagging efficiency $\epsilon_{i,c}$, and probability $\mathcal{P}_{i,c}$ over the M possible signal and background hypotheses i,

$$\mathcal{L}_c = \exp\left(-\sum_{i=1}^{M} n_i\epsilon_{i,c}\right)\prod_{j=1}^{N_c}\left[\sum_{i=1}^{M} n_i\epsilon_{i,c}\mathcal{P}_{i,c}(\vec{x}_j;\vec{\alpha}_i)\right]. \qquad (6)$$

Due to low statistics in the $\pi\pi$ channel, we fix the tagging efficiencies ϵ_i and fit for the total yield in each component, rather than directly determining the yield in each tagging category. The probabilities $\mathcal{P}_{i,c}$ are evaluated as the product of probability density functions (PDFs) for each of the independent variables $\vec{x}_j = \{m_{\rm ES}, \Delta E, \mathcal{F}, \theta_c^+, \theta_c^-, \Delta t\}$, where θ_c^+ and θ_c^- are the Cherenkov angles for the positive and negative tracks, respectively. The total likelihood is the product of likelihoods for each category and the parameters are determined by minimizing the quantity $-2\ln\mathcal{L}$.

The Δt PDF for signal $\pi^+\pi^-$ decays is given by Eq. 1, modified to include the dilution and dilution difference for each tagging category, and convolved with the signal resolution function. The Δt PDF for signal $K\pi$ events takes into account B^0–$\overline{B}^0$ mixing, depending on the charge of the kaon and the flavor of $B_{\rm tag}$. $B^0 \to K^+K^-$ decays are parameterized as an exponential convolved with the resolution function.

There are 18 free parameters in the fit:

- 3 signal and 3 background yields (n_i) for the $\pi\pi$, $K\pi$, and KK hypotheses.
- Signal and background charge asymmetries ($\mathcal{A}_{K\pi}$).
- 8 background parameters describing the shapes in $m_{\rm ES}$, ΔE, and $\mathcal{F}$.
- $S_{\pi\pi}$ and $C_{\pi\pi}$.

We fix the B lifetime τ and mixing frequency Δm_d to the PDG values [17].

6 Results

In a sample of 33 million $B\overline{B}$ pairs we find 65^{+12}_{-11} $\pi\pi$ and 217 ± 18 $K\pi$ events and measure the following CP parameters:

$$\begin{aligned} \mathcal{A}_{K\pi} &= -0.07 \pm 0.08 \pm 0.02, \\ S_{\pi\pi} &= 0.03^{+0.53}_{-0.56} \pm 0.11, \\ C_{\pi\pi} &= -0.25^{+0.45}_{-0.47} \pm 0.14, \end{aligned}$$

where the first error is statistical and the second is systematic. The correlation between $S_{\pi\pi}$ and $C_{\pi\pi}$ is -21%. Figure 2 shows distributions of $m_{\rm ES}$ and ΔE for events enhanced in signal $\pi^\pm\pi^\mp$ and $K^\pm\pi^\mp$ decays based on likelihood ratios. The likelihood for a given signal or background hypothesis is constructed from the yield, tagging efficiency, and the product of probabilities for $\mathcal{F}$, θ_c, and $m_{\rm ES}$ (ΔE) when plotting the projection for ΔE ($m_{\rm ES}$). The curves represent projections of the fit result scaled by the efficiency of the additional requirements. Figure 3 shows the Δt distribution for $\pi\pi$-enhanced events, with a looser selection than those applied in Fig. 2. The solid histogram represents the expected distribution for the selected sample, while the dashed histogram is the expected background shape. The core is consistent with the estimated composition of B decays and combinatorial background, and the tails are described well by the background resolution function.

6.1 Systematic uncertainties

Several sources contribute to the systematic error on $\mathcal{A}_{K\pi}$, $S_{\pi\pi}$, and $C_{\pi\pi}$:

- **PDFs for $m_{\rm ES}$, ΔE, $\mathcal{F}$.** We evaluate the systematic error on signal shapes with $B^- \to D^0\pi^-$ decays observed in data. We obtain the background shapes directly in the fit and, in addition, use an asymmetric Gaussian as an alternative parameterization for $\mathcal{F}$.

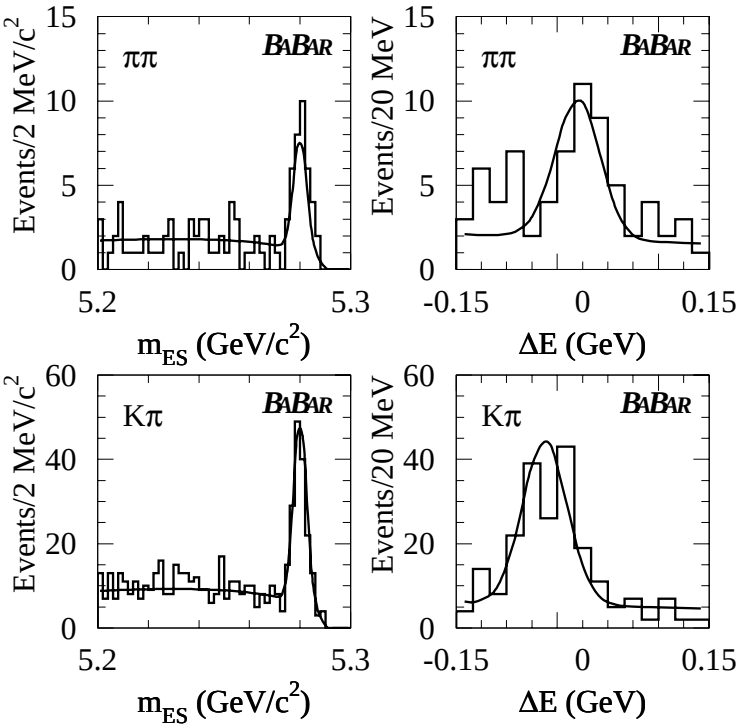

Figure 2: Distributions of $m_{\rm ES}$ and ΔE for events enhanced in signal $\pi^{\pm}\pi^{\mp}$ and $K^{\pm}\pi^{\mp}$ decays after likelihood ratio requirements. The solid curves represent projections of the maximum likelihood fit result after accounting for the efficiency of the additional requirements. The $\pi\pi \leftrightarrow K\pi$ cross-feed is estimated to be less than three events in each plot.

- **PDF for $\boldsymbol{\theta_c}$**. We vary the PDF parameters within conservative ranges.
- **Tagging**. We vary efficiencies, dilutions, and dilution differences within their errors. In addition, we compare tagging performance in simulated samples of $B_{\rm flav}$ and $\pi^+\pi^-$ decays, and repeat the maximum likelihhood fit with the background tagging efficiencies as free parameters.
- **PDFs for $\boldsymbol{\Delta t}$**. We vary all parameters of the signal and background resolution functions within their errors. In addition, to account for possible effects due to SVT misalignment, we exchange the parameters for 1999–2000 and 2001 data for both signal and background, which is a very conservative procedure. We also compare the results of fits using parameters obtained separately from the tagged and untagged $B_{\rm flav}$ samples.
- **$\boldsymbol{\tau}$ and $\boldsymbol{\Delta m_d}$**. We vary these parameters within the PDG errors [17].

Table 4 summarizes the systematic errors coming from all sources, and the total systematic error calculated as the sum in quadrature of the individual uncertainties.

6.2 Validation

Extensive studies using "toy" Monte Carlo, `GEANT` 3 Monte Carlo simulation, and data samples have been used to validate the fit technique. In large samples of toy Monte Carlo experiments generated with the statistics observed in the full dataset, we find no evidence of bias in any of the free parameters and the errors are consistent with expectations. The most probable errors are 0.59 and 0.41 for $S_{\pi\pi}$ and $C_{\pi\pi}$, respectively, consistent with the data fit results.

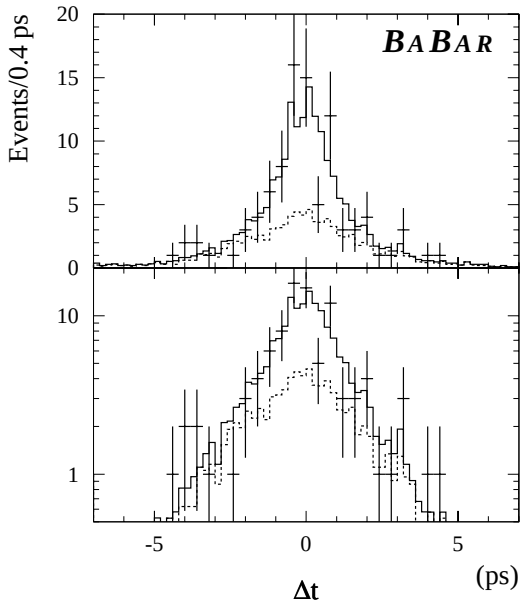

Figure 3: Distribution of Δt for a sample enhanced in $\pi^{\pm}\pi^{\mp}$ events obtained with likelihood ratio requirements. The solid histogram represents the expected distribution for signal and background, while the dashed histogram shows the expected background shape. The plot includes an estimated three $K\pi$ signal events.

Table 4: Summary of systematic errors from all sources. The total systematic error is calculated as the sum in quadrature of the individual uncertainties.

	$\mathcal{A}_{K\pi}$		$S_{\pi\pi}$		$C_{\pi\pi}$	
Source	$+$	$-$	$+$	$-$	$+$	$-$
$m_{\rm ES}$	0.003	0.002	0.007	0.005	0.018	0.022
ΔE	0.014	0.013	0.009	0.035	0.096	0.110
$\mathcal{F}$	0.007	0.007	0.024	0.024	0.046	0.046
θ_c	0.004	0.004	0.021	0.022	0.038	0.041
Sig Tagging	0.001	0.001	0.050	0.050	0.033	0.034
Bkg Tagging	0.001	0.001	0.007	0.006	0.009	0.009
Sig Δt	0.001	0.001	0.068	0.069	0.032	0.027
Bkg Δt	0.002	0.002	0.052	0.053	0.020	0.020
τ and Δm_d	0.000	0.000	0.011	0.011	0.007	0.007
Total	0.017	0.016	0.106	0.111	0.125	0.136

Fitting large samples of pure $\pi\pi$ and $K\pi$ simulated Monte Carlo events, we are able to extract the input values without bias when floating τ, Δm_d, $S_{\pi\pi}$, and $C_{\pi\pi}$. In samples of simulated signal and background Monte Carlo events equivalent $10\,\mathrm{fb}^{-1}$ we obtain consistent values of yields, τ, Δm_d, and the *CP* parameters, where the errors on the latter are in agreement with toy Monte Carlo predictions.

Fits to signal and background yields in the 1999–2000 and 2001 datasets without Δt information give results consistent with our branching fraction measurement [6], and we find consistent values of all fitted background parameters between the two datasets. Addition of Δt in the likelihood function improves the statistical error on $N_{\pi\pi}$ by approximately 9%, while the yield changes by only 1 event (1.5%).

As a validation of the Δt parameterization in data, we fit the full dataset to simultaneously extract yields, background parameters, τ, Δm_d, $S_{\pi\pi}$, and $C_{\pi\pi}$. We find $\tau = (1.52 \pm 0.12)\,\mathrm{ps}$ and $\Delta m_d = (0.54 \pm 0.09)\hbar\,\mathrm{ps}^{-1}$, and the remaining free parameters are stable with respect to the fit with fixed τ and Δm_d.

7 Summary

We have presented a preliminary measurement of the time-dependent *CP*-violating asymmetry in $B \to \pi^+\pi^-$ decays, and a preliminary updated measurement of the asymmetry between $B^0 \to K^+\pi^-$ and $\overline{B}^0 \to K^-\pi^+$ decays. In a sample of 33 million $B\overline{B}$ pairs we observe 65^{+12}_{-11} $\pi\pi$ and 217 ± 18 $K\pi$ candidates and measure the following parameters:

$$\begin{aligned} \mathcal{A}_{K\pi} &= -0.07 \pm 0.08 \pm 0.02, \\ S_{\pi\pi} &= 0.03^{+0.53}_{-0.56} \pm 0.11, \\ C_{\pi\pi} &= -0.25^{+0.45}_{-0.47} \pm 0.14, \end{aligned}$$

where the first error is statistical and the second is systematic. The systematic error on $\mathcal{A}_{K\pi}$ includes an uncertainty of ± 0.01 from possible charge bias in track reconstruction and particle identification. We observe no evidence for direct *CP* violation in $B \to K^\pm\pi^\mp$ decays, and calculate a 90% confidence limit on $\mathcal{A}_{K\pi}$ of $[-0.21, +0.07]$ assuming Gaussian errors. With the addition of more data and improvements in detector performance, measurements of $\mathcal{A}_{K\pi}$, $S_{\pi\pi}$, and $C_{\pi\pi}$ will yield increasingly more important information about *CP* violation in the B meson system.

8 Acknowledgments

We are grateful for the extraordinary contributions of our PEP-II colleagues in achieving the excellent luminosity and machine conditions that have made this work possible. The collaborating institutions wish to thank SLAC for its support and the kind hospitality extended to them. This work is supported by the US Department of Energy and National Science Foundation, the Natural Sciences and Engineering Research Council (Canada), Institute of High Energy Physics (China), the Commissariat à l'Energie Atomique and Institut National de Physique Nucléaire et de Physique des Particules (France), the Bundesministerium für Bildung und Forschung (Germany), the Istituto Nazionale di Fisica Nucleare (Italy), the Research Council of Norway, the Ministry of Science and Technology of the Russian Federation, and the Particle Physics and Astronomy Research Council (United Kingdom). Individuals have received support from the Swiss National Science Founda-

tion, the A. P. Sloan Foundation, the Research Corporation, and the Alexander von Humboldt Foundation.

References

[1] N. Cabibbo, Phys. Rev. Lett. **10**, 531 (1963); M. Kobayashi and T. Maskawa, Prog. Th. Phys. **49**, 652 (1973).

[2] *BABAR* Collaboration, B. Aubert *et al.*, hep-ex/0107013, submitted to Phys. Rev. Lett.

[3] BELLE Collaboration, K. Abe *et al.*, hep-ex/0107061, submitted to Phys. Rev. Lett.

[4] OPAL Collaboration, K. Ackerstaff *et al.*, Eur. Phys. Jour. C **5**, 379 (1998); CDF Collaboration, T. Affolder *et al.*, Phys. Rev. D **61**, 072005 (2000); ALEPH Collaboration, R. Barate *et al.*, Phys. Lett. B **492**, 259 (2000); BELLE Collaboration, A Abashian *et al.*, Phys. Rev. Lett. **86**, 2509 (2001); *BABAR* Collaboration, B. Aubert *et al.*, Phys. Rev. Lett. **86**, 2515 (2001).

[5] See, for example, F.J. Gilman, K. Kleinknecht and B. Renk, Eur. Phys. Jour. C **15**, 110 (2000).

[6] *BABAR* Collaboration, B. Aubert *et al.*, hep-ex/0105061, submitted to Phys. Rev. Lett.

[7] M. Beneke, G. Buchalla, M. Neubert, and C.T. Sachrajda, hep-ph/0104110 (2001).

[8] Y.Y. Keum, H-n. Li, and A.I. Sanda, Phys. Rev. D **63**, 054008 (2001).

[9] M. Gronau and D. London, Phys. Rev. Lett. **65**, 3381 (1990);

[10] N.G. Deshpande and X.G. He, Phys. Rev. Lett. **74**, 26 (1995); S. Gardner, Phys. Rev. D **59**, 077502 (1999).

[11] Y. Grossman and H.R. Quinn, Phys. Rev. D **58**, 017504 (1998); J. Charles, Phys. Rev. D **59**, 054007 (1999); M. Gronau, D. London, N. Sinha, and R. Sinha, hep-ph/0105308 (2001).

[12] *BABAR* Collaboration, B. Aubert *et al.*, *BABAR*-PUB-01/08, to appear in Nucl. Instrum. Methods.

[13] G. C. Fox and S. Wolfram, Nucl. Phys. B **149**, 413 (1979).

[14] S. L. Wu, Phys. Rep. **107**, 59 (1984).

[15] ARGUS Collaboration, H. Albrecht *et al.*, Z. Phys. C **48**, 543 (1990).

[16] *BABAR* Collaboration, B. Aubert *et al.*, hep-ex/0107036, submitted to this conference.

[17] D.E. Groom *et al.*, the Particle Data Group, *Review of Particle Physics*, Eur. Phys. Jour. C **15**, 1 (2000).